


 Cite this: *RSC Adv.*, 2021, **11**, 31727

## Optimization study on deep extractive oxidative desulfurization with tetrabutylammonium bromide/polyethylene glycol DES

Yanwen Guo, Xingjian Liu, Jingwen Li and Bing Hu\*

Green, efficient and inexpensive desulfurizing solvents have always been a considerable focus of petroleum desulfurization research. In this study, a series of deep eutectic solvents (DESs) based on tetrabutylammonium bromide (TBAB)/polyethylene glycol 200 (PEG-200) with different molar ratios were synthesized and characterized by Fourier transform infrared spectroscopy and  $^1\text{H}$  nuclear magnetic resonance spectroscopy. Dibenzothiophene (DBT) was removed deeply as the classic sulfide in model oil, and  $\text{H}_2\text{O}_2$  was fully utilized by the new TBAB/PEG-200 desulfurization system in step extractive oxidative desulfurization. The reaction conditions were optimized further, and O/S = 8, DES/oil = 1 : 5, 40 °C and 75 minutes were chosen as the best reaction conditions. Meanwhile, other organic sulfides in crude oil were also removed, and the removal rates of DBT, 4,6-dimethyldibenzothiophene and benzothiophene were 99.65%, 96.71% and 93.52%, respectively. The DES was reused 7 times, and the desulfurization efficiency of the regenerated DES for DBT was maintained at 98.14%. Finally, the possible mechanism of the synergistic effect of two kinds of hydrogen bonds and the oxidant was proposed.

Received 9th July 2021

Accepted 5th September 2021

DOI: 10.1039/d1ra05295k

[rsc.li/rsc-advances](http://rsc.li/rsc-advances)

## 1. Introduction

With the great progress of society and science, travel modes have become diversified. Meanwhile, the emission of sulfur compounds from all kinds of vehicles has caused serious harm to nature.<sup>1</sup> For example, acid rain has caused serious corrosion of trees, buildings, transportation pipelines and feed pumps, and it has also caused deactivation of chemical catalysts, death of fish and crops, and harm to humans. It is vital for the environment and living things to deeply remove sulfides from fuel oil. Consequently, many national governments have put forward exceedingly stringent requirements on the sulfur content in fuel.<sup>2</sup> The European Union strictly limited the sulfur content in fuel oil to less than 10 ppm in 2008. The China National V fuel standard was issued to reduce the sulfur content in gasoline to less than 10 ppm in 2016. The Environmental Protection Agency of the United States proposed that the minimum sulfur content in gasoline should be 10 ppm in 2017. Therefore, it is an urgent task to achieve deep desulfurization of fuel oil.

Many research groups have used numerous methods to solve this problem, such as hydrodesulfurization (HDS),<sup>3,4</sup> adsorptive desulfurization (ADS),<sup>5,6</sup> oxidative desulfurization (ODS),<sup>7,8</sup> extractive desulfurization (EDS)<sup>9,10</sup> and biological desulfurization (BDS).<sup>11,12</sup> Traditional HDS technology is widely used in industry because of its high removal efficiency for mercaptan, thioethers and disulfides, except for some aromatic sulfur compounds: thiophenes, benzothiophenes, and their derivatives. Hence, Ali *et al.*<sup>13</sup> synthesized

catalysts with carbon nanofiber-doped zeolite as a support and Mo-Co and Mo-Ni as active components to remove DBT from model oil by HDS. The results show that the synthesized catalyst had high stability and catalytic activity. The highest removal rate of DBT could reach 97.5% at 300 °C. However, the present HDS technology has the disadvantage of high energy consumption, expensive hydrogen materials, high temperature, high pressure and special catalyst requirements, which leads to high cost. Saleh<sup>14</sup> summarized that the reaction temperature of HDS was usually from 300 °C to 400 °C and the reaction pressure was generally from 50 to 100 bar. In addition, some nanomaterial catalysts are expensive, such as Pt-Rh nanoparticles/FSM 16. Hence, it is necessary to find less expensive and more efficient desulfurization technologies.

ODS and EDS have attracted researchers' increasing interest as efficient and effective methods owing to their mild operation conditions. For ODS,  $\text{H}_2\text{O}_2$  often plays the role of an inexpensive and efficient oxidant that cannot pollute the environment. Theoretically,  $\text{H}_2\text{O}_2$  could react with some polyoxometalates or heteropolyacids to produce corresponding species with higher activity, which would result in easier oxidation of organic sulfides. Rezvani *et al.*<sup>15</sup> synthesized a nanomaterial catalyst,  $\text{PMo}_{11}\text{Cu}@\text{MgCu}_2\text{O}_4@\text{CS}$ , for ODS.  $\text{H}_2\text{O}_2$ /acetic acid and acetonitrile were used as the oxidant and extractant, respectively. A highly active species, peroxyacetic acid, was obtained by the reaction of  $\text{H}_2\text{O}_2$  with acetic acid and was combined with the nanomaterial catalyst to attack sulfur atoms in the fuel. The organic sulfide was oxidized to the corresponding sulfones, which were extracted into acetonitrile. The results showed that the desulfurization system had excellent desulfurization efficiency of 97% for real oil under mild conditions. For EDS, traditional desulfurization

School of Materials and Chemical Engineering, Hubei University of Technology, Wuhan 430068, China



solvents included *N,N*-dimethylformamide, acetonitrile and dimethyl sulfoxide,<sup>16–18</sup> whose volatility is harmful to humans and the environment. Ionic liquids (ILs) address the shortcomings of traditional solvents due to their low volatility, high thermal stability, chemical stability, non-flammability and flexible designability. Accordingly, ILs have been used as a new kind of desulfurization extractant or catalyst since 2001.<sup>19</sup> Recently, ILs have made remarkable advancements in EDS and ODS, and the desulfurization efficiencies have been almost 100% under mild conditions.<sup>20–22</sup> However, ILs are toxic, poorly biodegradable, expensive and difficult to prepare, which limited their application in industry. DESs overcome these disadvantages of ILs due to their nontoxicity, low price, reasonable biodegradability and simple preparation processes. The properties of DESs are similar to those of ILs, and many DESs are easy to recycle as desulfurizing solvents.<sup>23–25</sup> A DES, a new class of alternative green solvent, is generally formed from two or three compounds by hydrogen bonding. The hydrogen bond acceptors (HBA) usually consist of quaternary ammonium salts. Polyols, urea and carboxylic acids usually act as hydrogen bond donors (HBD). DESs were first proposed by Abbott's research team.<sup>26</sup> They were not formally employed in the desulfurization field until 2013.<sup>27</sup> In recent years, DESs have been intensively studied in separation of substances,<sup>28</sup> electrochemistry,<sup>29</sup> preparation of nanomaterials,<sup>30</sup> synthesis of cellulose and its derivatives, and other research fields.<sup>31</sup> A DES is usually liquid at room temperature, and it can play the roles of extractant and catalyst. Therefore, heterocyclic organic sulfides can be extracted from the oil phase to a DES phase by hydrogen bonds combined with sulfur atoms. Studies show that hydrogen bonding is the main driving force, and the removal of sulfur atoms is also affected by CH–π, π–π and metal coordination.<sup>32–34</sup>

The advantages of PEG are good water solubility, low volatility, non-toxicity and varying molar mass. Especially, low molar mass PEGs have been widely employed in industry as environmentally friendly solvents. As HBDs in DESs, many kinds of DESs have been applied to desulfurization by researchers. For example, Majid *et al.*<sup>35</sup> chose PEG-400 as the HBD and tetrabutylammonium chloride (TBAC) as the HBA to synthesize DESs with different molar ratios. The removal rate of DBT was 79.01% when the volume ratio of DES to model oil was 1 : 1 at 25 °C. It is significant to promote the development of EDS with PEG-based DESs. The probabilities of intermolecular collision increase due to hydrogen bonding, high temperature, fast mixing speed and other factors. However, H<sub>2</sub>O<sub>2</sub>

may also decompose quickly in this condition, which can result in the loss of oxidant. To solve this problem, some groups proposed the step reaction method. Diana *et al.*<sup>36</sup> prepared two kinds of DESs, PEG-200/TBAC and PEG-200/choline chloride (CHCl). The DESs were used as extractants and two kinds of molybdenum complexes were used as catalysts for extractive catalytic oxidative desulfurization. In the first step, the DES and simulated oil were stirred for 10 minutes for EDS. In the second step, the oxidant was added to the desulfurization system for simultaneous EDS and ODS. The results show that the desulfurization efficiencies of simulated oil with a sulfur content of 3000 ppm could reach more than 90% in one hour and 100% in two hours with 0.75 ml PEG/CHCl, 0.35 mmol H<sub>2</sub>O<sub>2</sub> and 10 μmol catalyst at 70 °C. In addition, real diesel oil was desulphurized, and the desulfurization efficiency reached 82%. Additionally, PEG can be used as a desulfurization extractant alone. Kianpour *et al.*<sup>37</sup> used PEG to reduce the content of DBT in simulated oil from 512 ppm to less than 10 ppm.

To solve the problem of harsh conditions in HDS, the relatively expensive raw materials of ILs and the loss of H<sub>2</sub>O<sub>2</sub> in catalytic oxidative desulfurization, TBAB and PEG-200 were selected as the raw materials of a DES according to previous studies. Both TBAB and TBAC can also be used as phase transfer catalysts and ion pair reagents,<sup>38–41</sup> but the cost of TBAB is lower than that of its counterpart. Hence, TBAB/PEG-200 DESs with different molar ratios were synthesized by using PEG-200 as the HBD and TBAB as the HBA and characterized by Fourier transform infrared (FT-IR) spectroscopy and <sup>1</sup>H nuclear magnetic resonance (<sup>1</sup>H NMR) spectroscopy. According to the mechanism of extractive coupled oxidative desulfurization,<sup>42–44</sup> the DESs were used in desulfurization by a step reaction. In order to test the desulfurization performance of DES TBAB/PEG-200, the effects of different temperatures, O/S molar ratios, DES/oil volume ratios, additives and sulfur compounds on the desulfurization efficiency and the capacities of regenerating and recycling were investigated with control variates by adding extractant and oxidant to the reactor at different times. Finally, the probable mechanism of step extractive oxidative desulfurization was proposed.

## 2. Experimental

### 2.1 Materials

The reagents used in the research were not purified shown in the Table 1.

Table 1 Information about the principal reagents used in this research

Chemical	Abbreviation	Purity (wt%)	CAS number	Supplier
Tetrabutylammonium bromide	TBAB	99.0	1643-19-2	Shanghai Macklin Biochemical Co., Ltd
Polyethylene glycol 200	PEG-200	98.0	25322-68-3	Sinopharm Chemical Reagent Co., Ltd
Octane		98.0	111-65-9	Sinopharm Chemical Reagent Co., Ltd
Dibenzothiophene	DBT	98.0	132-65-0	Shanghai Macklin Biochemical Co., Ltd
1-Benzothiophene	BT	97.0	95-15-8	Shanghai Macklin Biochemical Co., Ltd
4,6-Dimethyl dibenzothiophene	4,6-DBT	97.0	1207-12-1	Shanghai Macklin Biochemical Co., Ltd
Hydrogen peroxide	H <sub>2</sub> O <sub>2</sub>	30.0	7722-84-1	Sinopharm Chemical Reagent Co., Ltd
Cyclohexene		99.0	110-83-8	Shanghai Macklin Biochemical Co., Ltd
Toluene		99.5	108-88-3	Shanghai Sigma Aldrich Trade Co., Ltd
Pyridine		99.5	110-86-1	Shanghai Macklin Biochemical Co., Ltd



## 2.2 Preparation of the model oil

A certain amount of heterocyclic organic sulfide was dissolved in *n*-octane and transferred into a volumetric flask. The mass of organic sulfur in the model oil with a sulfur content of 500 ppm followed formula (1):

$$500 \times 10^{-6} = 32 \times m_{\text{OS}} / (M_{\text{OS}} \times V_{\text{oil}}) \quad (1)$$

Here,  $m_{\text{OS}}$  (g),  $M_{\text{OS}}$  (g mol<sup>-1</sup>) and  $V_{\text{oil}}$  (ml) are the mass of organic sulfur, molar mass of organic sulfur and total volume of model oil, respectively. As a typical example, in the preparation method of 500 ppm DBT model oil, 0.2879 g DBT was dissolved in *n*-octane and transferred into a 100 ml volumetric flask.

## 2.3 Preparation and characterization of the DESs

The syntheses of the TBAB/PEG-200 DESs were carried out in a round bottom flask with vigorous stirring at 80 °C for 100 minutes. For example, when the mole ratio of TBAB and PEG-200 was 1 : 2, 4.5132 g of solid TBAB was taken with an electronic balance and 5 ml of liquid PEG-200 was taken with a 5 ml sampler. DESs with different molar ratios were successfully prepared until uniform and transparent liquids were obtained.

The synthesized DESs were characterized exclusively by FT-IR and <sup>1</sup>H NMR spectroscopy. The functional groups and formation of hydrogen bonds in the DESs were analyzed by a Nicolet 6700 FT-IR spectrometer (Thermo Fisher, Waltham, MA, USA) using potassium bromide tablets. <sup>1</sup>H NMR spectroscopy was utilized to evaluate the effects of the hydrogen bonds formed in the different DESs. The specification of the nuclear magnetic resonance spectrometer was Bruker 400M (Karlsruhe, Germany), and D<sub>2</sub>O was used as the solvent.

## 2.4 Extractive and oxidative desulfurization process of the model oil

A certain amount of model oil was added to a round bottom flask. Several milliliters of DES were added to the model oil and stirred to perform the extraction reaction first. After 15 minutes, a proper amount of upper oil was taken out by micropipette to determine the performance of extractive desulfurization; then, H<sub>2</sub>O<sub>2</sub> was added to the reaction system to oxidize the sulfur. After that, sampling was carried out every 15 minutes. The calculation of the desulfurization efficiency was in accord with formula (2):

$$R (\%) = (C_0 - C_1) / C_0 \times 100\% \quad (2)$$

where  $R$ ,  $C_0$  (ppm) and  $C_1$  (ppm) stand for the desulfurization efficiency and the concentrations of sulfide before and after removal, respectively. The upper oil sample was measured by a gas chromatography-flame ionization detector (GC-FID) (VF-1 column type; 30 m × 0.25 mm × 0.25 μm; column temperature: 230 °C; raised from 100 °C to 230 °C at the rate of 20 °C min<sup>-1</sup> and maintained for 6 minutes; injector port temperature: 250 °C; detector temperature: 300 °C).

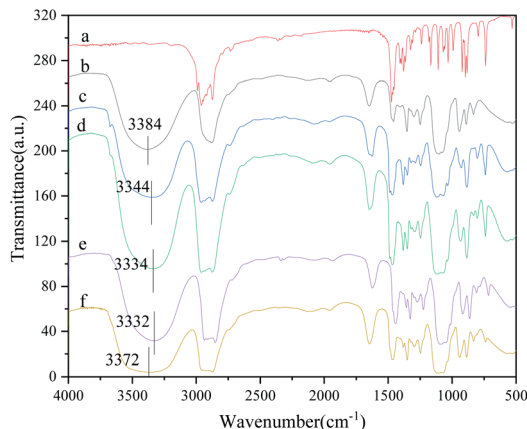


Fig. 1 FT-IR spectra of TBAB, PEG-200 and TBAB/PEG-200 with different molar ratios: (a) TBAB, (b) PEG-200, (c) TBAB/PEG-200 = 2 : 1, (d) TBAB/PEG-200 = 1 : 1, (e) TBAB/PEG-200 = 1 : 2 and (f) TBAB/PEG-200 = 1 : 3.

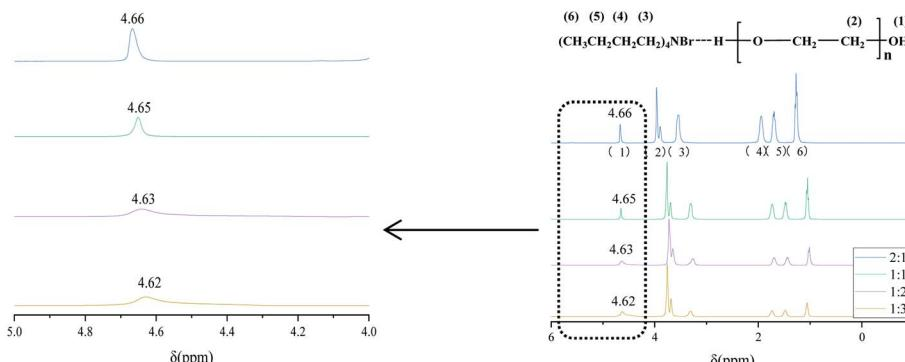
## 3 Results and discussion

### 3.1 Characterization of DES TBAB/PEG-200

The infrared curves of TBAB, PEG-200 and TBAB/PEG-200 with different molar ratios are shown in Fig. 1 to investigate the interaction between TBAB and PEG-200. The results show that the peaks for the C-H and C-O-C stretching vibration, C-O stretching vibration and O-H bond bending vibration in PEG-200 were at 2875 cm<sup>-1</sup>, 1105 cm<sup>-1</sup> and 925 cm<sup>-1</sup>, respectively. The peaks at 2956 cm<sup>-1</sup>, 1473 cm<sup>-1</sup> and 1110 cm<sup>-1</sup> were attributed to the stretching vibration of C-H, the bending vibration of C-H and the stretching vibration of C-N in TBAB, respectively. In fact, when the H atom is combined with an atom with high electronegativity by a covalent interaction, the common electron pair is strongly attracted to the atom with high electronegativity. Hence, the H atom with some positive charge could be combined with another atom with high electronegativity to form a hydrogen bond. The formation of hydrogen bonds could result in an average density of the electron cloud, which resulted in a reduction of the frequency of the stretching vibration. The DES contained N, O and Br atoms with high electronegativity; therefore, the field of force around the H atom in O-H caused by these atoms changed. Above all, the characteristic stretching vibration of the O-H bond in PEG-200 was from 3090 cm<sup>-1</sup> to 3710 cm<sup>-1</sup>, but the wavelengths of the DESs were wider. Different redshifts of O-H from 3384 cm<sup>-1</sup> to 3344 cm<sup>-1</sup>, 3334 cm<sup>-1</sup>, 3332 cm<sup>-1</sup> and 3372 cm<sup>-1</sup> also proved the existence of hydrogen bonds. With the increase of PEG-200, the effect of hydrogen bonding first increased and then decreased. When the molar ratio of TBAB to PEG-200 was 1 : 3, the formation of hydrogen bonds lacked the corresponding HBA, which resulted in a decrease of the red shift value. The desulfurization efficiency showed an identical trend, which first went upward and then downward.

In order to further study the relationship of the hydrogen bonds between PEG-200 and TBAB, the <sup>1</sup>H NMR spectra of the DESs are presented in Fig. 2. For the different DESs, the H



Fig. 2  $^1\text{H}$  NMR spectra of TBAB/PEG-200.

chemical shifts of  $-\text{OH}$  varied from 4.66 ppm to 4.62 ppm. Furthermore, the shapes of the peaks became wider and shorter. The shapes of the peaks were similar when the molar ratio was 1 : 2 and 1 : 3. Specially, two kinds of hydrogen bonds,  $\text{O}-\text{H}\cdots\text{N}$  and  $\text{O}-\text{H}\cdots\text{Br}$ , are proposed in this paper because of the existence of highly electronegative N and Br atoms in TBAB. The electronegativity of N was higher, so the electron screening effect was more noticeable, and the bond energy of  $\text{O}-\text{H}\cdots\text{N}$  was higher than that of  $\text{Br}$ .<sup>45</sup> Due to the existence of hydrogen bonding, the signal of hydrogen in TBAB also had different effects, and the area of the peak decreased. All the above evidence demonstrated that different DESs with driving forces of hydrogen bonding were successfully obtained.

### 3.2 Influence of the DES on the desulfurization efficiency

Prepared DESs with different molar ratios of HBD to HBA were used to explore the preliminary desulfurization effect of the model oil, as shown in Table 2. When only PEG-200 was used as the extractant, the desulfurization efficiency reached 71.47% because of weak hydrogen bonds arising between the sulfur atom in DBT and  $\text{O}-\text{H}$  in PEG-200. The desulfurization effect was inferior to that described in the literature.<sup>37</sup> In the processes of synthesizing a series of DESs, it could be observed that the fluidity of the DESs was poor at room temperature when the molar ratio of TBAB to PEG-200 was 2 : 1 or 1 : 1. Under such conditions, the desulfurization efficiencies were low, and they were 82.13% and 83.67%, respectively. The highest desulfurization efficiency of 93.92% could be obtained when the molar ratio of TBAB/PEG-200 was 1 : 2. The desulfurization

Table 2 Desulfurization efficiencies of the different DESs<sup>a</sup>

Entry	TBAB : PEG-200	Desulfurization efficiency (%)
1	0 : 5	71.47
2	2 : 1	82.13
3	1 : 1	83.67
4	1 : 2	93.92
5	1 : 3	88.02

<sup>a</sup> Reaction condition: 5 ml DBT model oil, 5 ml DES, O/S = 8, 40 °C, 75 min.

efficiencies increased with the decrease of the TBAB/PEG-200 molar ratio from 2 : 1 to 1 : 2, which followed the decrease of the chemical shift of H in the  $^1\text{H}$  NMR spectrum. Meanwhile, excessive solid TBAB formed a liquid with high viscosity, which slowed the chemical kinetics and decreased the reaction rate. On the other hand, when the molar ratio of TBAB/PEG-200 was 1 : 3, the desulfurization efficiency was reduced to 88.02%. This may have occurred because excess PEG-200 diluted the concentrations of DES and  $\text{H}_2\text{O}_2$ , reducing the strength of the hydrogen bonds and the catalytic oxidation ability.

### 3.3 Influence of temperature on the desulfurization efficiency

It can be seen from Fig. 3 that the desulfurization rate increased with the increase of temperature in the first 15 minutes. The desulfurization efficiency was not very high at 20 °C. The main reason may be that the oxidation capacity of the active oxygen components was too low to show great desulfurization performance at this temperature. Another reason may be that the force between the hydrogen bonds and sulfur atoms in DBT was

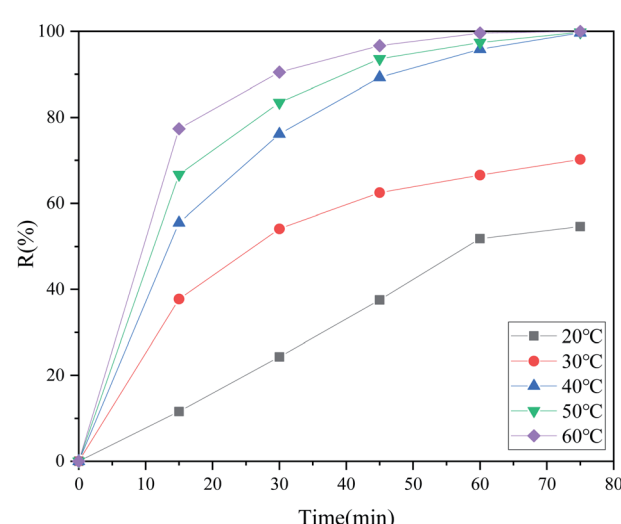


Fig. 3 Changes in the desulfurization efficiency with the reaction time at different temperatures (2 ml DES, 10 ml DBT model oil, O/S = 8).



too weak at relatively low room temperature, and most of the DBT remained in the upper oil phase. When the temperature was raised to 30 °C or 40 °C, the desulfurization efficiencies significantly improved in the first 15 minutes. The desulfurization efficiency could reach 55.51% after extractive reaction at 40 °C. This is because only hydrogen bonding was the driving force in the extraction stage. After adding H<sub>2</sub>O<sub>2</sub> to the round bottom flask, the desulfurization efficiency was improved obviously and could reach over 76.16% in 30 minutes. After 75 minutes, the desulfurization efficiency could be over 99.65%, which meant that the sulfur content of the 500 ppm model oil was below 10 ppm. During the extractive oxidative reaction, the power of DBT conversion was derived from the synergistic action of hydrogen bonding and oxidation. The desulfurization efficiency increased with increasing reaction temperature, which can be attributed to the stronger binding forces between the hydrogen bonds and S atoms in this temperature range. Nevertheless, the desulfurization efficiencies in 75 minutes did not change much with increasing temperature. This may be because the reaction almost reached equilibrium, or a trace amount of H<sub>2</sub>O<sub>2</sub> was decomposed into O<sub>2</sub> with low oxidation activity at 50 °C or 60 °C. The following reactions were completed at the mild temperature of 40 °C, which could decrease the expenditure of energy in industry.

#### 3.4 Influence of the O/S molar ratio on the desulfurization efficiency

In fact, 1 mol DBT is theoretically needed to react with 1 mol H<sub>2</sub>O<sub>2</sub>, and a slight excess of oxidant can promote the oxidation reaction. It can be obtained from Fig. 4 that the sulfur removal rate of 15 minute extractive desulfurization reached about 54.38% without adding oxidant. When the O/S molar ratio was 2, the desulfurization efficiency at 75 minutes was very low, and it was only 74.72%. This is because the H<sub>2</sub>O<sub>2</sub> added was not enough to oxidize too much DBT, and the force of

desulfurization was mainly extraction by the hydrogen bonding between the DES and the S atoms in DBT. With the addition of sufficient H<sub>2</sub>O<sub>2</sub>, the DBT originally existing in the DES phase was oxidized to dibenzothiophene sulfoxide (DBTO) or dibenzothiophene sulfone (DBTO<sub>2</sub>), and the DBT in the oil phase was extracted to the DES phase continuously. Therefore, the desulfurization efficiency started to increase as more H<sub>2</sub>O<sub>2</sub> was added. When the O/S molar ratio was greater than 4, the desulfurization efficiency increased obviously and could reach 99.65% due to the synergistic effect of sufficient oxidant and the hydrogen bonding force; therefore, DBT was almost completely removed to achieve deep desulfurization. Accordingly, when the O/S molar ratio increased to 10, the desulfurization rate did not increase significantly. This might have been because the oxidation reaction of DBT had reached equilibrium. Moreover, the addition of H<sub>2</sub>O<sub>2</sub> introduced a small amount of water, which could dilute the DES and result in weakening of the intermolecular hydrogen bond forces.<sup>46</sup> Hence, an O/S ratio of 8 was selected as the best reaction condition for the following reactions due to its excellent desulfurization efficiency in the same time.

#### 3.5 Influence of the DES/oil volume ratio on the desulfurization efficiency

If a small amount of solvent can purify more crude oil, it will be more economical in industry. As plotted in Fig. 5, the sulfur removal of DBT was only 85.32% when the volume ratio of DES to model oil was 1 : 10. Upon increasing the volume ratio to 1 : 5 and 2 : 5, the desulfurization efficiencies could reach 99.65% and 99.70%, respectively. The reason was that more DES could help to extract more DBT in the upper phase and oxidize that in the lower phase. However, the desulfurization efficiency decreased marginally when the volume ratio was increased to 3 : 5. The reason may be that the excessive DES diluted the concentration of H<sub>2</sub>O<sub>2</sub>.<sup>47</sup> Hence, the volume ratio of 1 : 5 was

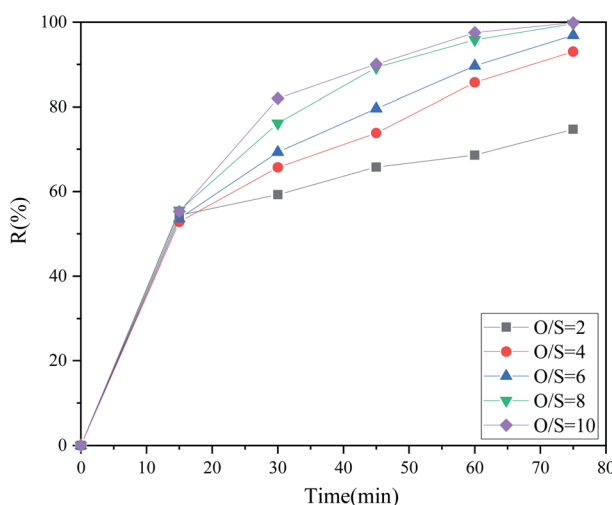


Fig. 4 Changes in the desulfurization efficiency with the reaction time with different molar ratios of oxidant to sulfide (2 ml DES, 10 ml DBT model oil, 40 °C).

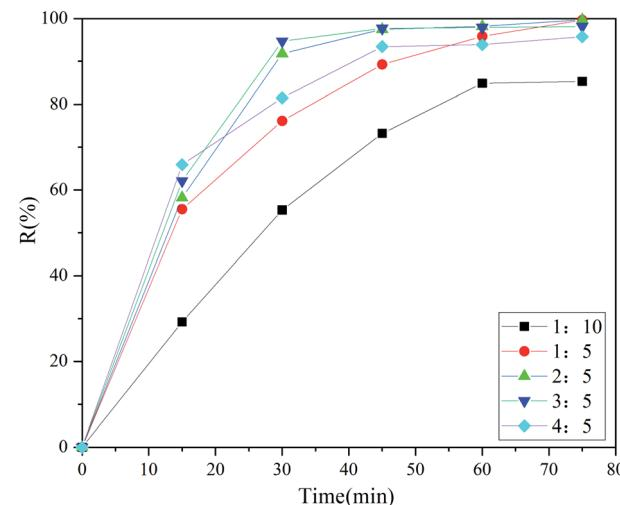


Fig. 5 Changes in the desulfurization efficiency with the reaction time at different volume ratios of DES to oil (10 ml DBT model oil, O/S = 8, 40 °C).



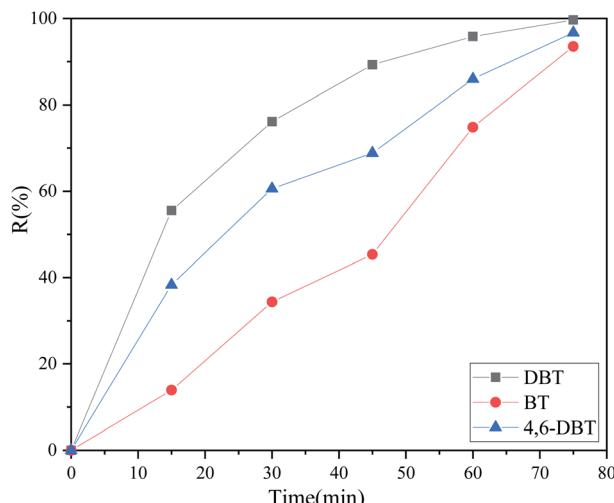


Fig. 6 Changes in the desulfurization efficiency with the reaction time for different kinds of sulfides (2 ml DES, 10 ml model oil, O/S = 8, 40 °C).

used as the most suitable condition in this experiment. Specially, it can be seen from the above data that the desulfurization efficiencies increased gradually with the increase of the dose of DES in 15 minutes. This occurred because more DES could provide more extractive active sites which could attack S atoms. However, the force of hydrogen bonding alone could not remove all DBT completely from the oil phase in the short time of 15 minutes. Hence, many researchers adopted the approaches of multi-stage extraction or extraction coupled with oxidation to perform desulfurization and obtained great results.<sup>48–51</sup>

### 3.6 Influence of sulfur compounds on the desulfurization efficiency

In addition to DBT, other typical sulfides in real oil were removed as heterocyclic organic sulfides under the optimum

reaction conditions. As pictured in Fig. 6, the removal rates of DBT, BT and 4,6-DBT reached 99.65%, 96.71% and 93.52%, respectively. DBT could be removed more effectively than the other two sulfur compounds in this way. DBT contained two benzene rings and had high electron cloud density; therefore, the sulfur atoms could be more easily activated and extracted by hydrogen bonds. According to previous literature reports, the electron densities on the sulfur atom of 4,6-DBT, DBT and BT are 5.760, 5.758 and 5.739, respectively.<sup>52,53</sup> Although 4,6-DBT had a higher electron cloud than DBT, the conversion efficiency was slightly lower than that of DBT. This can be attributed to the increase of steric hindrance due to the presence of two methyl groups, which hindered the formation of hydrogen and the combination of oxygen with sulfur atoms. There is only one benzene ring in BT, but the sulfur atom is difficult to activate due to its lower electron density.

### 3.7 Influence of the addition of cycloparaffin, aromatic, olefin and heterocyclic nitrogen compounds on the desulfurization efficiency

Due to the complex compositions in real diesel, cycloparaffin, aromatic, olefin and heterocyclic nitrogen compounds were added to the model oil as additives to test their influence on the new desulfurization system. 100 ml of the *n*-octane multicomponent model oil contained hydrocarbon compounds, namely 5 ml cyclohexene, 5 ml cyclohexane and 5 ml toluene, and 250 ppm pyrrole and 500 ppm DBT were used as heterocyclic compounds. Fig. 7 shows that the desulfurization rate in 75 minutes decreased from 99.65% to 96.93% compared with the DBT model oil, which may be due to the participation of some oxidants in the ring-opening reaction of cyclohexene or the oxidation reaction of pyridine.<sup>54</sup> However, the desulfurization rate changed from 55.51% to 55.22% at 15 minutes, which indicated that the addition of the complex compounds had little effect on the extractive desulfurization.

### 3.8 Influence of the reaction method on the desulfurization efficiency

As is listed in Table 3, the sulfur removals of DBT, BT and 4,6-DBT were very low without oxidant, only 84.16%, 71.91% and 80.07%, respectively. Therefore, deep desulfurization could not be achieved by only extraction. When H<sub>2</sub>O<sub>2</sub> was used in the desulfurization process, the sulfur removal rates increased sharply. The reason may be that the heterocyclic organic

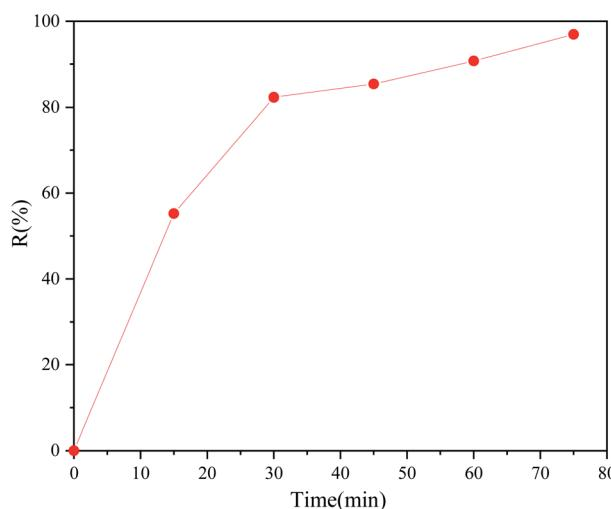


Fig. 7 Changes in the desulfurization efficiency with the reaction time for other complex components (2 ml DES, 10 ml multicomponent model oil, O/S = 8, 40 °C).

Table 3 Comparison of different desulfurization methods<sup>a</sup>

Sulfide	Desulfurization efficiency (%)		
	No oxidant	Conventional process	Step reaction
DBT	84.16	94.59	99.65
BT	71.91	88.28	93.52
4,6-DBT	80.07	89.22	96.71

<sup>a</sup> Reaction condition: 2 ml DES, 10 ml model oil, O/S = 8, 40 °C, 75 min.



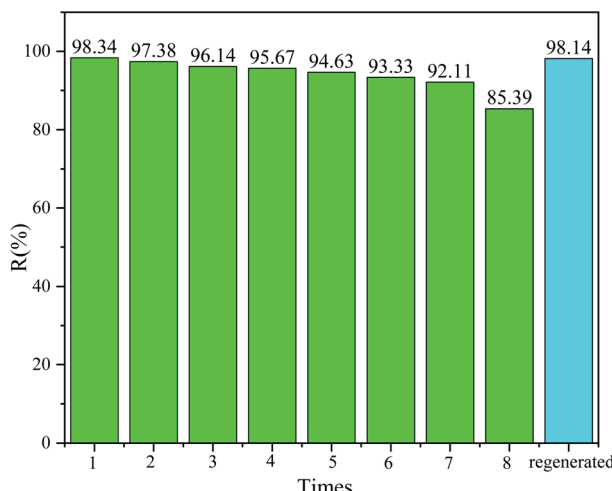


Fig. 8 Recycling and regeneration performance (2 ml DES, 10 ml DBT model oil, O/S = 8, 40 °C, 75 min).

sulfides were oxidized to the corresponding sulfones with strong polarity, and more sulfides could be extracted from the oil into the TBAB/PEG-200 DES. In order to explore the effect of step extractive oxidative desulfurization, the desulfurization efficiencies of the different reaction processes were compared. When model oil, DES and oxidant were added to the reactor at the same time, the conversion efficiencies of DBT, BT and 4,6-DBT were 94.59%, 88.28% and 89.22%, respectively. Under the optimized program, the desulfurization efficiencies increased by 5.06%, 5.24% and 7.49%, respectively. A possible reason is that the former method accelerated the consumption of some H<sub>2</sub>O<sub>2</sub>. Some H<sub>2</sub>O<sub>2</sub> could be decomposed into H<sub>2</sub>O and O<sub>2</sub> under the action of stirring, heating or other conditions. During the

upward movement of oxygen molecules, most of the oxygen was lost; thus, the pressure in the reactor increased, and only a small part of oxygen was used for oxidative desulfurization (see Fig. 11). In brief, the first extraction could reduce unnecessary loss of H<sub>2</sub>O<sub>2</sub> and improve the sulfur removal rate.

### 3.9 DES recycling

In addition to high desulfurization efficiency, recyclability and reusability are important evaluation criteria for the applicability of DES TBAB/PEG-200, which is in line with sustainable development of the economy. In order to explore the recycling performance of the DES, several sets of cyclic tests were conducted under the optimized reaction conditions. The cycle study is shown in Fig. 8. After seven cycles, the desulfurization efficiency was still above 92.11%. However, the desulfurization efficiency started to decrease obviously in the eighth cycle. The primary cause could be that DES was nearly saturated and the desulfurization capacity was reduced greatly. Likewise, a trace amount of water which came from H<sub>2</sub>O<sub>2</sub> after each cycle could weaken the hydrogen bonding abilities between DES and DBT. After the reaction solution was divided into water and oil phases by decantation, the DES could be regenerated and purified by water washing, filtering, rotary evaporation and vacuum drying. Firstly, the oil and water phases were separated by a separating funnel. The water phase was discharged from the bottom of the separating funnel, and the upper layer was the product oil. Secondly, a white solid precipitated because of the different solubilities of sulfide in the two kinds of liquids when water was added to the aqueous phase. The solid was filtered after standing for some time. Thirdly, the residual water in DES was removed by a rotary evaporator at 90 °C. The regenerated DES was reused for the new desulfurization system, and the

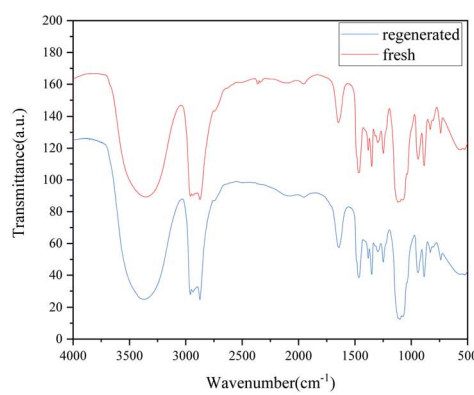


Fig. 9 FT-IR and <sup>1</sup>H NMR spectra of fresh and regenerated DES.

Table 4 Details of desulfurization compared with previous literature reports

DES	Method	T (°C)	O/S	DES/oil	Recyclability	R (%)	Ref.
TBAC : PEG-400 = 1 : 1	Extractive	25		1 : 1		79.59	33
TBAC : PEG = 1 : 2	Extractive	25		2 : 1	5	82.83	38
TBAB : PEG-600 = 1 : 2	Extractive	25		1 : 1	5	82.40	55
TBAB : PEG-200 = 1 : 2	Extractive and oxidative	40	8 : 1	1 : 5	7	99.65	This paper



Table 5 Prices of the HBDs and HBAs

Chemicals	PEG-200	PEG-400	PEG-600	TBAC	TBAB
Price (¥)	8.40/kg	9.40/kg	9.70/kg	72.00/kg	12.00/kg

desulfurization efficiency could reach 98.14%. The FT-IR and  $^1\text{H}$  NMR spectra of the regenerative DES were compared with those of fresh DES. It can be seen from Fig. 9 that they changed slightly, which indicated that the DES possessed a stable structure and great regeneration performance.

### 3.10 Comparison of the desulfurization efficiency with previous literature

Table 4 depicts the comparison of different desulfurization information between other literature reports and this paper. In terms of reaction temperature, the temperature used in this study was slightly higher than that used in the other three reports. However, the amount of DES was the smallest. Higher desulfurization efficiency was obtained by adding a small amount of oxidant and without multiple extraction reactions. The recyclability was also better than that of the other two schemes. In the

other three literature reports, deep desulfurization was achieved by three-stage extraction, but the cost of the equipment and operation process increased. As shown in Table 5, the costs of PEG-200 and TBAB used in this paper were both lower. The prices were based on Guide Chemical and Alibaba and changed moderately. Based on the comprehensive analyses, the desulfurization system proposed in this paper was more economical.

### 3.11 Mechanism of step extractive oxidative desulfurization

According to the studies in previous literature reports, one of the mechanisms of extractive coupled oxidative desulfurization is that DBT is extracted into the aqueous phase by the interaction of the extractant and DBT, and then the sulfur in the aqueous phase is oxidized and removed. In this paper, the method of adding extractant and oxidant in two stages was adopted. As far as DBT was concerned, DBT was combined with the DES TBAB/PEG-200 to enter the lower phase solution by 15 minute extractive desulfurization. When  $\text{H}_2\text{O}_2$  was not used, the removal of S mainly depended on the forces of hydrogen bonding of  $\text{O}-\text{H}\cdots\text{N}$  and  $\text{O}-\text{H}\cdots\text{Br}$  bonds, as shown in Fig. 10. With the addition of  $\text{H}_2\text{O}_2$ , the sulfide in the lower layer was oxidized and the sulfide in the upper was extracted into the

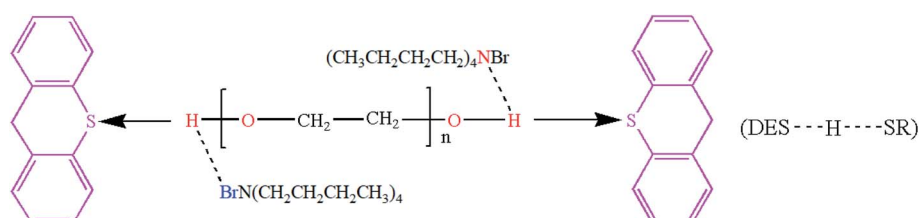
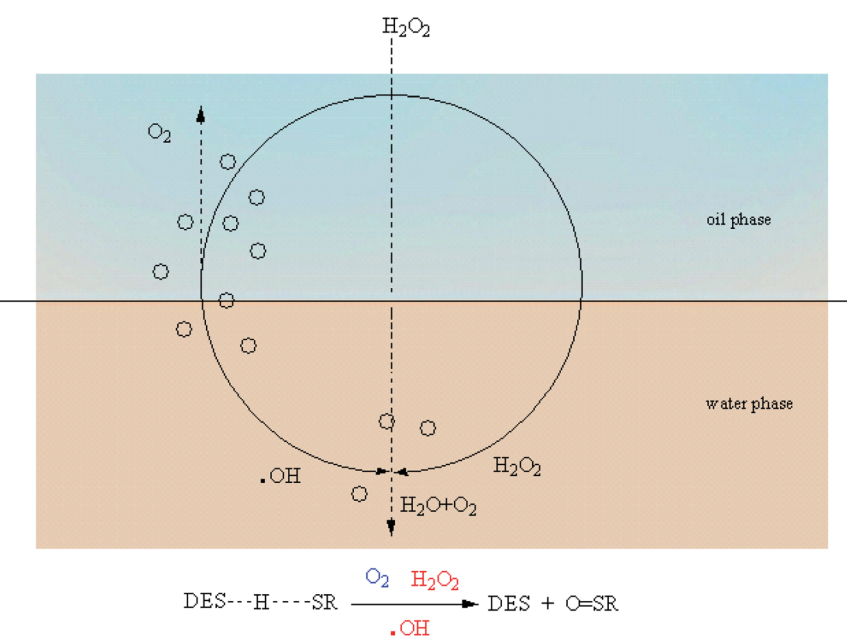


Fig. 10 The combination of DES and DBT (SR stands for DBT).

Fig. 11 The pathway of  $\text{H}_2\text{O}_2$  and oxidation of DBT (O = SR stands for DBTO or DBTO<sub>2</sub>).

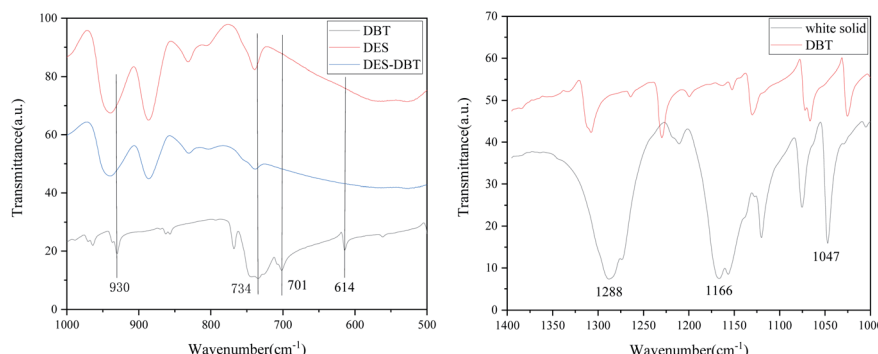


Fig. 12 FT-IR spectra of DBT, the white solid, fresh DES and DBT-DES.

lower solution simultaneously. It is speculated that  $\text{H}_2\text{O}_2$  was divided into two parts in the desulfurization system, as shown in Fig. 11. First, some  $\text{H}_2\text{O}_2$  was converted into 'OH with high activity under the catalysis of DES and then reacted with DBT. Second, when the TBAB in DES played the role of phase transfer catalyst, additional  $\text{H}_2\text{O}_2$  was brought into the two phases in an agitated state by TBAB and reacted with DBT directly. Hence, DBT was oxidized to the corresponding sulfoxide or sulfone under the synergistic effect of hydrogen bonding and oxidization and was removed easily from the aqueous phase. Accordingly, the step extractive oxidative reaction could further increase the desulfurization efficiency because  $\text{H}_2\text{O}_2$  was fully utilized and the loss of  $\text{H}_2\text{O}_2$  was reduced by the new desulfurization system. In order to explore the mechanism ulteriorly, the white solid dissolved in DES phase was obtained and characterized by FT-IR, as shown in Fig. 12. According to the peaks at  $1288\text{ cm}^{-1}$ ,  $1166\text{ cm}^{-1}$  and  $1047\text{ cm}^{-1}$ , it was speculated that the solid might contain DBTO, DBTO<sub>2</sub> and DBT that was not oxidized. Meanwhile, some characteristic peaks of the benzene ring in DBT from  $1000\text{ cm}^{-1}$  to  $500\text{ cm}^{-1}$  weakened and disappeared. This may be due to the fact that the electron donor group in DES weakened the aromaticity of DBT, which enabled DBT to be oxidized easily. Moreover, no other substance was detected in the upper oil, as shown in Fig. 13, which indicated that product oil with relatively high purity was obtained.

## 4. Conclusions

In this paper, TBAB/PEG-200 DESs with different molar ratios were synthesized and characterized by FT-IR and <sup>1</sup>H NMR spectroscopy. The results showed that a series of TBAB/PEG-200 DESs with H bonds were successfully prepared and applied to step extractive oxidative desulfurization. The representative heterocyclic organic sulfide DBT in model oil was used to explore the appropriate molar ratio of TBAB and PEG-200. According to the experiments, higher desulfurization efficiency could be obtained when TBAB/PEG-200 = 1 : 2. The optimum reaction conditions of the DES were further explored by the method of control variates. The results show that the removal rate of DBT could reach 99.65% when the temperature was 40 °C, the molar ratio of  $\text{H}_2\text{O}_2$  to DBT was 8 and the volume ratio of DES to oil was 1 : 5. Different desulfurization procedures were compared under the optimized reaction conditions, and the step extractive oxidative desulfurization used in this paper showed the best sulfur removal performance. It is inferred that the decomposition of  $\text{H}_2\text{O}_2$  can be reduced by step extractive oxidative desulfurization. Two other typical heterocyclic sulfur compounds were also removed, and the desulfurization efficiencies of 4,6-DBT and BT were 96.71% and 93.53%, respectively. Other alkane, olefin, aromatic and nitrogen heterocyclic compounds were also added to the DBT model oil, and the desulfurization rate of DBT decreased from 99.65% to 96.93%, which shows that the desulfurization rate was not greatly affected by these compounds. The fresh DES was not treated and could be used 7 times. Meanwhile, it can be seen from the FT-IR and <sup>1</sup>H NMR spectra of the fresh and regenerated DES that the DES had high stability, and the desulfurization rate for DBT model oil could still reach more than 98.14%. Compared with other literature reports, the new desulfurization system was more applicable. For the mechanism of stage extractive oxidative desulfurization, the possible force of DBT removal is the extraction of DBT by hydrogen bonding in DES and the oxidation of DBT by TBAB in DES as a catalyst and  $\text{H}_2\text{O}_2$  as an oxidant. The solid separated from DES also proved that DBT was oxidized to the corresponding DBTO<sub>2</sub> in the desulfurization process. In summary, the improved desulfurization program could be employed in the removal of

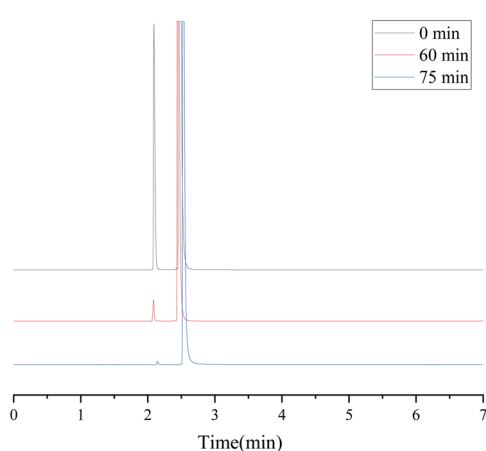


Fig. 13 GC-FID of the upper oil at different reaction times.



fuel oil as an efficient strategy. It is expected to achieve industrialization because of its economy and efficiency.

## Author contributions

Yanwen Guo and Bing Hu conceived and designed the experiments. Yanwen Guo performed the experiments. Yanwen Guo, Xingjian Liu, Jingwen Li and Bing Hu analysed the data. Yanwen Guo, Xingjian Liu and Bing Hu wrote the manuscript. Jingwen Li and Bing Hu supervised the project.

## Conflicts of interest

The authors declare no competing financial interest.

## Acknowledgements

This study has been partially financed by Hubei Natural Science Foundation Project (2013CKB032) and the Doctoral Program of Hubei University of Technology (200701).

## References

- 1 L. Alves, S. M. Paixão, R. Pacheco, *et al.*, Biodesulphurization of fossil fuels: energy, emissions and cost analysis, *RSC Adv.*, 2015, **5**, 34047–34057.
- 2 M. F. Majid, H. F. M. Zaid, C. F. Kait, *et al.*, Futuristic advance and perspective of deep eutectic solvent for extractive desulfurization of fuel oil: A review, *J. Mol. Liq.*, 2020, **306**, 112870.
- 3 T. A. Saleh, S. A. AL-Hammadi and A. M. Al-Amer, Effect of boron on the efficiency of MoCo catalysts supported on alumina for the hydrodesulfurization of liquid fuels, *Process Saf. Environ. Prot.*, 2019, **121**, 165–174.
- 4 H. A. Al-Jamimi and T. A. Saleh, Transparent predictive modelling of catalytic hydrodesulfurization using an interval type-2 fuzzy logic, *J. Cleaner Prod.*, 2019, **231**, 1079–1088.
- 5 T. A. Saleh, Simultaneous adsorptive desulfurization of diesel fuel over bimetallic nanoparticles loaded on activated carbon, *J. Cleaner Prod.*, 2018, **172**, 2123–2132.
- 6 B. Qin, Y. Shen, B. Xu, *et al.*, Mesoporous  $\text{TiO}_2\text{-SiO}_2$  adsorbent for ultra-deep desulfurization of organic-S at room temperature and atmospheric pressure, *RSC Adv.*, 2018, **8**(14), 7579–7587.
- 7 M. A. Rezvani, P. Afshari and M. Aghmasheh, Deep catalytic oxidative desulfurization process catalyzed by TBA-PWFe@NiO@BNT composite material as an efficient and recyclable phase-transfer nanocatalyst, *Mater. Chem. Phys.*, 2021, **267**, 124662.
- 8 M. A. Rezvani, M. A. N. Asli, M. Oveis, *et al.*, An organic-inorganic hybrid based on an Anderson-type polyoxometalate immobilized on PVA as a reusable and efficient nanocatalyst for oxidative desulphurization of gasoline, *RSC Adv.*, 2016, **6**, 53069–53079.
- 9 A. N. El-hoshoudy, F. S. Soliman and D. M. Abd El-Aty, Extractive desulfurization using choline chloride-based DES/molybdate nanofluids; Experimental and theoretical investigation, *J. Mol. Liq.*, 2020, **318**, 114307.
- 10 F. A. Hatab, A. S. Darwish, T. Lemaoui, *et al.*, Extraction of Thiophene, Pyridine, and Toluene from n-Decane as a Diesel Model Using Betaine-Based Natural Deep Eutectic Solvents, *J. Chem. Eng. Data*, 2020, **65**, 5443–5457.
- 11 W. Li, M. Zhang, D. Kang, *et al.*, Mechanisms of sulfur selection and sulfur secretion in a biological sulfide removal (BISURE) system, *Environ. Int.*, 2020, **137**, 105549.
- 12 M. Fernández, M. Ramírez, J. M. Gómez, *et al.*, Biogas biodesulfurization in an anoxic biotrickling filter packed with open-pore polyurethane foam, *J. Hazard. Mater.*, 2014, **264**, 529–535.
- 13 I. Ali, A. A. Al-Arfaj and T. A. Saleh, Carbon nanofiber-doped zeolite as support for molybdenum based catalysts for enhanced hydrodesulfurization of dibenzothiophene, *J. Mol. Liq.*, 2020, **304**, 112376.
- 14 T. A. Saleh, Characterization, determination and elimination technologies for sulfur from petroleum: Toward cleaner fuel and a safe environment, *Trends Environ. Anal. Chem.*, 2020, **25**, e00080.
- 15 M. A. Rezvani, M. Shaterian, Z. S. Aghbolagh, *et al.*, Synthesis and Characterization of New Inorganic-Organic Hybrid Nanocomposite  $\text{PMo}_{11}\text{Cu}@\text{MgCu}_2\text{O}_4@\text{CS}$  as an Efficient Heterogeneous Nanocatalyst for ODS of Real Fuel, *ChemistrySelect*, 2019, **4**, 6370–6376.
- 16 Y. Gao, Z. Liu, R. Gao, *et al.*, Support ionic liquid-heteropolyacid hybrid on mesoporous carbon aerogel with a high surface area for highly efficient desulfurization under mild conditions, *Microporous Mesoporous Mater.*, 2020, **305**, 110392.
- 17 A. M. Viana, D. Julião, F. Mirante, *et al.*, Straightforward activation of metal-organic framework UiO-66 for oxidative desulfurization processes, *Catal. Today*, 2021, **362**, 28–34.
- 18 U. Maity, J. K. Basu and S. Sengupta, Performance study of extraction and oxidation-extraction coupling processes in the removal of thiophenic compounds, *Fuel Process. Technol.*, 2014, **121**, 119–124.
- 19 A. Bösmann, L. Datsevich, A. Jess, *et al.*, Deep desulfurization of diesel fuel by extraction with ionic liquids, *Chem. Commun.*, 2001, 2494–2495.
- 20 A. M. Kermani, V. Mahmoodi, M. Ghahramaninezhad, *et al.*, Highly efficient and green catalyst of {Mo132} nanoballs supported on ionic liquid-functionalized magnetic silica nanoparticles for oxidative desulfurization of dibenzothiophene, *Sep. Purif. Technol.*, 2021, **258**, 117960.
- 21 Y. Gao, Z. Lv, R. Gao, *et al.*, Dawson type polyoxometalate based-poly ionic liquid supported on different carbon materials for high-efficiency oxidative desulfurization with molecular oxygen as the oxidant, *New J. Chem.*, 2020, **44**, 20358–20366.
- 22 Q. Wu, Q. Shi, J. Shang, *et al.*, Synthesis of Surface-Active Heteropolyacid-Based Ionic Liquids and Their Catalytic Performance for Desulfurization of Fuel Oils, *ACS Omega*, 2020, **5**, 31171–31179.
- 23 J. Yin, J. Wang, Z. Li, *et al.*, Deep desulfurization of fuels based on an oxidation/extraction process with acidic deep eutectic solvents, *Green Chem.*, 2015, **17**, 4552–4559.



24 W. Liu, T. Li, G. Yu, *et al.*, One-pot oxidative desulfurization of fuels using dual-acidic deep eutectic solvents, *Fuel*, 2020, **265**, 116967.

25 F. Lima, J. Gouvenaux, L. C. Branco, *et al.*, Towards a sulfur clean fuel: Deep extraction of thiophene and dibenzothiophene using polyethylene glycol-based deep eutectic solvents, *Fuel*, 2018, **234**, 414–421.

26 A. P. Abbott, G. Capper, D. L. Davies, *et al.*, Preparation of novel, moisture-stable, Lewis-acidic ionic liquids containing quaternary ammonium salts with functional side chains, *Chem. Commun.*, 2001, 2010–2011.

27 C. Li, D. Li, S. Zou, *et al.*, Extraction desulfurization process of fuels with ammonium-based deep eutectic solvents, *Green Chem.*, 2013, **15**, 2793–2799.

28 F. Bai, C. Hua and J. Li, Separation of Benzene-Cyclohexane Azeotropes via Extractive Distillation Using Deep Eutectic Solvents as Entrainers, *Processes*, 2021, **9**, 336.

29 T. M. Abdel-Fattah and J. D. Loftis, Comparison of Electropolishing of Aluminum in a Deep Eutectic Medium and Acidic Electrolyte, *Molecules*, 2020, **25**, 5712.

30 Z. Wang, T. Wu, J. Ru, *et al.*, Eco-friendly preparation of nanocrystalline Fe-Cr alloy coating by electrodeposition in deep eutectic solvent without any additives for anti-corrosion, *Surf. Coat. Technol.*, 2021, **406**, 126636.

31 E. Jakubowska, M. Gierszewska, J. Nowaczyk, *et al.*, The role of a deep eutectic solvent in changes of physicochemical and antioxidative properties of chitosan-based films, *Carbohydr. Polym.*, 2021, **255**, 117527.

32 W. Jiang, H. Li, C. Wang, *et al.*, Synthesis of ionic-liquid-based deep eutectic solvents for extractive desulfurization of fuel, *Energy Fuels*, 2016, **30**, 8164–8170.

33 M. Razavian and S. Fatemi, Intensified Transformation of Low-Value Residual Fuel Oil to Light Fuels with TPABr: EG as Deep Eutectic Solvent with Dual Functionality at Moderate Temperatures, *Energy Fuels*, 2020, **34**, 5497–5510.

34 C. Li, J. Zhang, Z. Li, *et al.*, Extraction desulfurization of fuels with 'metal ions' based deep eutectic solvents (MDESS), *Green Chem.*, 2016, **18**, 3789–3795.

35 M. Majid, H. F. Mohd Zaid, C. Fai Kait, *et al.*, Liquid polymer eutectic mixture for integrated extractive-oxidative desulfurization of fuel oil: An optimization study via response surface methodology, *Processes*, 2020, **8**, 848.

36 D. Julião, A. C. Gomes, M. Pillinger, *et al.*, Desulfurization of diesel by extraction coupled with Mo-catalyzed sulfoxidation in polyethylene glycol-based deep eutectic solvents, *J. Mol. Liq.*, 2020, **309**, 113093.

37 E. Kianpour and S. Azizian, Polyethylene glycol as a green solvent for effective extractive desulfurization of liquid fuel at ambient conditions, *Fuel*, 2014, **137**, 36–40.

38 H. Ito, Determination of Nitrate Ion Concentration in Fresh Vegetable Juices Using Ion-Pair Ultra Performance Liquid Chromatography (IP-UPLC), *JARQ*, 2016, **50**, 45–48.

39 X. Li, G. Li, H. Chang, *et al.*, Tetrabutylammonium bromide-mediated ring opening reactions of N-tosylaziridines with carboxylic acids in DMF, *RSC Adv.*, 2014, **4**(13), 6490–6495.

40 B. K. Banik, B. Banerjee, G. Kaur, *et al.*, Tetrabutylammonium Bromide (TBAB) Catalyzed Synthesis of Bioactive Heterocycles, *Molecules*, 2020, **25**, 5918.

41 Y. Zhang, F. Xing and S. Zhu, Structures and Chromogenic Ion-Pair Recognition of a Catechol-Functionalized 1, 8-Anthraquinone Macrocycle in Dimethyl Sulfoxide, *Inorg. Chem.*, 2021, **60**, 5042–5053.

42 W. Jiang, K. Zhu, H. Li, *et al.*, Synergistic effect of dual Brønsted acidic deep eutectic solvents for oxidative desulfurization of diesel fuel, *Chem. Eng. J.*, 2020, **394**, 124831.

43 L. Hao, M. Wang, W. Shan, *et al.*, L-proline-based deep eutectic solvents (DESS) for deep catalytic oxidative desulfurization (ODS) of diesel, *J. Hazard. Mater.*, 2017, **339**, 216–222.

44 C. Li, D. Li, S. Zou, *et al.*, Extraction desulfurization process of fuels with ammonium-based deep eutectic solvents, *Green Chem.*, 2013, **15**, 2793–2799.

45 M. K. Hadj-Kali, S. Mulyono, H. F. Hizaddin, *et al.*, Removal of thiophene from mixtures with n-heptane by selective extraction using deep eutectic solvents, *Ind. Eng. Chem. Res.*, 2016, **55**, 8415–8423.

46 H. Lü, P. Li, Y. Liu, *et al.*, Synthesis of a hybrid Anderson-type polyoxometalate in deep eutectic solvents (DESS) for deep desulphurization of model diesel in ionic liquids (ILs), *Chem. Eng. J.*, 2017, **313**, 1004–1009.

47 J. Xu, Z. Zhu, T. Su, *et al.*, Green aerobic oxidative desulfurization of diesel by constructing an Fe-Anderson type polyoxometalate and benzene sulfonic acid-based deep eutectic solvent biomimetic cycle, *Chin. J. Catal.*, 2020, **41**, 868–876.

48 A. Rajendran, H. X. Fan, T. Y. Cui, *et al.*, Enrichment of polymeric  $WO_x$  species in  $WO_x@SnO_2$  catalysts for ultra-deep oxidative desulfurization of liquid fuels, *Fuel*, 2021, **290**, 120036.

49 N. Sudhir, P. Yadav, B. R. Nautiyal, *et al.*, Extractive desulfurization of fuel with methyltriphenyl phosphonium bromide-tetraethylene glycol-based eutectic solvents, *Sep. Sci. Technol.*, 2020, **55**, 554–563.

50 J. Li, Y. Guo, J. Tan, *et al.*, Polyoxometalate Dicationic Ionic Liquids as Catalyst for Extractive Coupled Catalytic Oxidative Desulfurization, *Catalysts*, 2021, **11**, 356.

51 H. Liu, S. Chen, X. Li, *et al.*, Preparation of [EMIM]DEP/2C<sub>3</sub>H<sub>4</sub>O<sub>4</sub> DESS and its oxidative desulfurization performance, *Sep. Sci. Technol.*, 2021, **56**, 558–566.

52 Y. Zhu, M. Zhu, L. Kang, *et al.*, Phosphotungstic acid supported on mesoporous graphitic carbon nitride as catalyst for oxidative desulfurization of fuel, *Ind. Eng. Chem. Res.*, 2015, **54**, 2040–2047.

53 S. Otsuki, T. Nonaka, N. Takashima, *et al.*, Oxidative desulfurization of light gas oil and vacuum gas oil by oxidation and solvent extraction, *Energy Fuels*, 2000, **14**, 1232–1239.

54 C. Wang, Z. Chen, X. Yao, *et al.*, Decavanadates anchored into micropores of graphene-like boron nitride: Efficient heterogeneous catalysts for aerobic oxidative desulfurization, *Fuel*, 2018, **230**, 104–112.

55 W. S. A. Rahma, F. S. Mjalli, T. Al-Wahaibi, *et al.*, Polymeric-based deep eutectic solvents for effective extractive desulfurization of liquid fuel at ambient conditions, *Chem. Eng. Res. Des.*, 2017, **120**, 271–283.

